



Conjugate Natural Convection in a Square Porous Cavity Filled with a Nanofluid in the Presence of Two Isothermal Cylindrical Sources

Islam Bouafia^{1,*}, Razli Mehdaoui², Syham Kadri^{2,3}, Mohammed Elmir^{1,2}

¹ Mechanical Modeling and Experimentation Laboratory, Tahri Mohamed University, Bechar 08000, Algeria

² Energarid Laboratory, Tahri Mohamed University, Bechar 08000, Algeria

³ Laboratory of Semiconductor Devices Physics, Tahri Mohamed University, Bechar 08000, Algeria

ARTICLE INFO

Article history:

Received 5 October 2020

Received in revised form 12 November 2020

Accepted 12 November 2020

Available online 5 February 2021

ABSTRACT

In this work, a numerical study has been performed for the problem of steady-state natural convection in a square porous cavity having solid wall of finite thickness and conductivity filled by a nanofluid in the presence of two isothermal cylindrical sources. The external walls of the cavity are considered adiabatic and the circular sources are maintained at hot and cold uniform temperature. The internal thick wall has been a conducting solid. The governing dimensionless equations are solved using Galerkin finite element method and Darcy-Brinkman model assumed to be adopted. The results are presented as isotherms, streamlines, stream function values, average and local Nusselt number for various combinations of Rayleigh and Darcy numbers, concentration of nanoparticles, Thermal conductivity ratio and dimensionless wall thickness of the solid portion. The convection heat transfer can be enhanced by increasing of these parameters except for the wall thickness.

Keywords:

free convection; conduction heat transfer; porous medium; nanofluid; cylindrical source; Galerkin finite element method

1. Introduction

Study of free convection heat transfer in porous media filled by nanofluid is a very interesting topic in engineering applications, for example: solar energy, heat exchangers, thermal buildings, electronic cooling and geophysics. We can cite a review of Khanafer *et al.*, [1] and Kasaeian *et al.*, [2]. Many theoretical and experimental investigations have been realized in this domain, we quote about that Sheikhzadeh and Nazari [4] have studied the steady state natural convection in porous medium saturated with (Al₂O₃-Water) inside differentially heated square cavity [3-15]. The governing equations have solved by finite volume approach using SIMPLER algorithm. They showed the effect

*Corresponding author.

E-mail address: islambouafia9321@gmail.com

<https://doi.org/10.37934/arfmts.80.1.147164>

of Rayleigh number, Darcy number and nanoparticles volume fraction on the heat transfer. They concluded that the increase of these parameters increases the heat transfer. Baïri [5] has realized the experimental studies of natural convection in a tilted hemispherical enclosure filled by water-ZnO nanofluid saturated by porous materials. They have found the heat transfer enhances with increasing of nanofluid volume fraction and thermal conductivity of porous medium. Abdelraheem Aly [6] has been realized a numerical analysis of natural convection over circular cylinders in a porous enclosure filled with a nanofluid under thermo-diffusion effects. The effects of Rayleigh number, Darcy parameter, Soret number with modified Dufour number and nanoparticles parameters in heat and mass transfer have studied. Pop *et al.*, [7] and Groşan *et al.*, [8] have focused on the investigation of the steady natural convection in a two-dimensional porous square cavity saturated with a nanofluid, the transport equations are solved numerically using the finite difference method, the mathematical model of Buongiorno's has been adopted. Those considered the effect of Rayleigh number, Lewis number and the dimensionless ratio between the thermophoretic and Brownian coefficients on the thermal heat transfer. Dogonchi *et al.*, [9] and Hussain and Rahomey [10] have presented a numerical analysis of free convection in a nanofluid-saturated porous annulus developed with different geometries (circular; triangular; elliptic; rectangular; rhombic and square). The governing equations have solved by finite element method. In all cases, an increment in Rayleigh and Darcy numbers expand the heat transfer and average Nusselt number. Also, Hussain and Rahomey [10] has been showed the efficiency of difference geometries inside a square porous cavity. The effect of magnetohydrodynamic natural convection in a nanofluid-porous annulus area has been studied by Sheikholeslami and Shehzad [11], Sheikholeslami *et al.*, [12] and Ahmed *et al.*, [13].

In other hands, conjugate natural convection in a square porous cavity saturated with nanofluid has a various scope in industries as, in the design and construction of buildings, heat exchangers and storage of different types of energy. Conjugate heat transfer in a porous cavity filled with nanofluids containing a heated triangular thick wall has been studied by Chamkha and Ismael [16], they noted the effect of Rayleigh number, wall thickness, volume fraction of nanoparticles and the conductivity of solid partition on the Nusselt number. The governing equations have solved by over-successive relaxation finite-difference method. In this field the impact of Conjugate heat transfer and entropy generation has been demonstrated by Ismael *et al.*, [17] and Alsabery *et al.*, [18] investigated a numerical study of finite wavy wall thickness on entropy generation in the case of natural convection in cavity partially filled with non-Darcy porous layer in the presence of alumina nanoparticles. The system of partial differential equations has solved numerically with finite element method. The effect of Darcy number, porosity of the porous layer, number of undulations and the nanoparticles volume fraction are studied. They have showed that the Nusselt number increase with augmentation of the four influencing parameters. Sheremet and Pop [19] takes into account the Brownian diffusion and thermophoresis effects on conjugate natural convection in a square porous cavity filled by a nanofluid using Buongiorno's mathematical model. Mehryan *et al.*, [20] has been focused a numerical study in the case of conjugate problem within a porous square enclosure occupied with micropolar nanofluid using local thermal non-equilibrium model (LTNE). The transport equations are solved numerically using Galerkin finite element method in a non-uniform grid. In this field Ghalambaz *et al.*, [21] have detected the effect of hybrid nanofluid in the presence of Ag-MgO nanoparticles, the local thermal non-equilibrium model has been adopted. The problem of three difference layer (solid portion, porous layer and free nanofluid) has been investigated by Tahmasebi *et al.*, [22], Mehryan *et al.*, [23] and Ismael and Chamkha [24]. From these studies, we have shown the effect of several parameters such as: the Rayleigh and Darcy number, the thickness of the solid layer, the concentration of nanoparticles and the effect of the wall thermal conductivity.

Based on the above review, the objective of this paper is to investigate numerically the steady-state conjugate natural convection heat transfer in a porous cavity filled by nanofluid in the presence of two isothermal cylindrical sources. Following our bibliographic research, there are no works in the literature, which treat this subject despite its importance in several applications (specification of the originality of our paper). In the physical configuration, we considered the effect of two different isothermal sources with insulated cavity in the presence of conducting solid partition of finite thickness, therefore, the Darcy-Brinkman model is applied for simulated the viscous flow in the porous medium and the Boussinesq approximation for the buoyancy force. The aim of the study is to analyze the effect of several parameters such as The Rayleigh and Darcy Numbers, the thickness of conducting partition, the conductivity ratio and concentration of solid nanoparticles, in order to find the favorable storage and exchange condition of thermal energy.

2. Geometry and Mathematical Formulation

The physical model in this study is conjugate free convection-conduction in a porous square cavity of dimension ($H \times H$) saturated with alumina/ H_2O nanofluid in the presence of conducting solid with different thickness ε (see Figure 1). All external walls have been considered adiabatic and the two cylindrical geometries are maintained at different temperature (T_h and T_c). The nanofluid in the enclosure is assumed Newtonian and incompressible fluid. The porous domain is treated as to be uniform and undeformable. Also, the base fluid (H_2O) and the nanoparticles (Al_2O_3) are in thermal equilibrium. The solid matrix, nanofluid and the conductive portion are isotropic substance (see Table 1). In this work, we studied the laminar flow in homogeneous partitions, the thermal equilibrium between the nanofluid and the solid matrix is assumed to exist and the Boussinesq approximation has been adopted. The radiation effects, Brownian motion of nanoparticles and chemical reactions during flow are considered negligible.

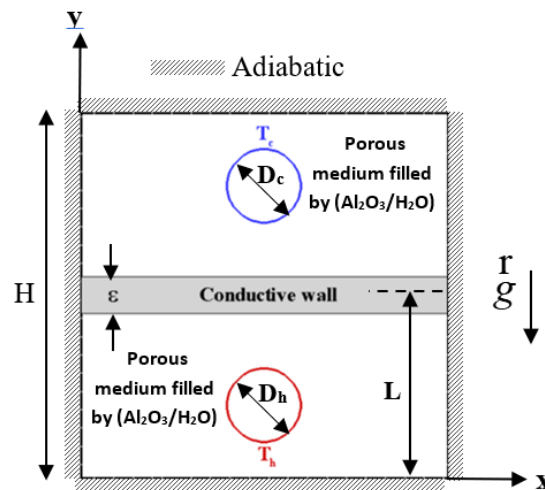


Fig. 1. Sketched of physical model

Based on the suspension theory, the effective density, the heat capacity and the thermal expansion coefficient of a nanofluid are calculated by the following formulas

$$\rho_{nf} = (1 - \phi)\rho_f + \phi\rho_s \quad (1)$$

$$(\rho c_p)_{nf} = (1 - \phi)(\rho c_p)_f + \phi(\rho c_p)_s \quad (2)$$

$$\beta_{nf} = (1 - \phi)\beta_f + \phi\beta_s \quad (3)$$

The effective thermal conductivity is approximated by semi-empirical model correlation based on experimental results [25]

$$k_{nf} = k_f(-13\phi^2 - 6.3\phi + 1) \quad (4)$$

The dynamic viscosity is calculated respectively from the Brinkmann model

$$\mu_{nf} = \frac{\mu_f}{(1-\phi)^{2.5}} \quad (5)$$

The thermal diffusivity of the nanofluid α_{nf} is deduced from

$$\alpha_{nf} = \frac{k_{nf}}{(\rho c_p)_{nf}} \quad (6)$$

Table 1

Thermophysical properties of water and nanoparticles at T=25°C [4]

Physical property	Water	Nanoparticles
Cp [J/Kg]	4179	765
ρ [Kg/m ³]	997.1	3960
k [W/m k]	0.613	40
β [K-1]	21x10 ⁻⁵	0.85x10 ⁻⁵
μ [kg/m.s]	8.55x10 ⁻⁴	-----

The Prandtl number of water equal to 5.83 [4]. In order to transform the governing equation into a dimensionless form, the following dimensionless variables are described

$$X = \frac{x}{H}; Y = \frac{y}{H}; U = \frac{uH}{\alpha_f}; V = \frac{vH}{\alpha_f}; P = \frac{pH^2}{\rho_{nf}\alpha_f^2}; \theta = \frac{T-T_c}{T_h-T_c} \quad (7)$$

The governing equations (mass, momentum and energy) for a steady, laminar and incompressible flow are as follows

$$\frac{\partial U}{\partial X} + \frac{\partial V}{\partial Y} = 0 \quad (8)$$

$$\frac{1}{(1-\phi)^{2.5}} \frac{Pr}{Da} U + \frac{\partial P}{\partial X} = \frac{1}{(1-\phi)^{2.5}} Pr \left(\frac{\partial^2 U}{\partial X^2} + \frac{\partial^2 U}{\partial Y^2} \right) \quad (9)$$

$$\frac{1}{(1-\phi)^{2.5}} \frac{Pr}{Da} V + \frac{\partial P}{\partial Y} = \frac{1}{(1-\phi)^{2.5}} Pr \left(\frac{\partial^2 V}{\partial X^2} + \frac{\partial^2 V}{\partial Y^2} \right) + Ra * Pr \left[(1 - \phi) + \phi \frac{\rho_s \beta_s}{\rho_f \beta_f} \right] \theta \quad (10)$$

$$(1 - \delta) \left[U \frac{\partial \theta}{\partial X} + V \frac{\partial \theta}{\partial Y} - k_r \alpha_r \left(\frac{\partial^2 \theta}{\partial X^2} + \frac{\partial^2 \theta}{\partial Y^2} \right) \right] = \delta \left[k_r \left(\frac{\partial^2 \theta}{\partial X^2} + \frac{\partial^2 \theta}{\partial Y^2} \right) \right] \quad (11)$$

We note here that for Porous domain saturated with nanofluid $\delta = 0$ and for Solid partition $\delta = 1$. Where the Rayleigh number Ra, Darcy number, conductivity and thermal diffusivity ratios are defined, respectively, as

$$Ra = \frac{\rho_f \beta_f H^3 g (T_h - T_c)}{\mu_f \alpha_f}; Da = \frac{K}{H^2}; k_r = \frac{k_w}{k_{nf}}; k_{r''} = \frac{k_p}{k_{nf}}; \alpha_r = \frac{\alpha_{nf}}{\alpha_f} \quad (12)$$

The centers of circular cylinders are located at (X=0.5H, Y=0.2H) for the hot cylinder and (X=0.5H, Y=0.8H) for the cold cylinder, the solid block has been taking place in the middle of enclosure, the dimensionless forms of the boundary conditions for the present problem are specified as follows

At the top cylinder

$$U=0, V=0, \theta = 0 \quad (13)$$

At the bottom cylinder

$$U=0, V=0, \theta = 1 \quad (14)$$

On all cavity sidewalls

$$U=0, V=0, \frac{\partial \theta}{\partial X} = \frac{\partial \theta}{\partial Y} = 0 \quad (15)$$

At the borders of a conductive partition

$$U=0, V=0, \frac{\partial \theta_w}{\partial n} = k_r \frac{\partial \theta}{\partial n} \quad (16)$$

The local Nusselt number is obtained from the following relation, where n is the unit normal coordinates to the surface of the wall.

$$Nu_l = \frac{k_{nf}}{k_f} \frac{\partial \theta}{\partial n} \Big|_{Wall} \quad (17)$$

The average Nusselt number at the hot cylinder is calculated by integrating the local Nusselt number along this wall.

$$Nu_{avr} = \frac{1}{\pi A} \int_0^{\pi A} Nu_l dn \quad (18)$$

3. Numerical Method and Code Validation

In the present computation, the obtained systems of algebraic Eq. (8)-(11) with the boundary conditions in Eq. (13)-(16) are discretized and solved by Galerkin finite element method, respectively. Lagrange-quadratic interpolation has been chosen. The normalized residuals of the momentum and energy equations became less than 10^{-6} .

In order to validate the numerical results, two different problems are considered. In the improved code the first test case is natural convection in porous media filled by alumina nanofluid with left heated wall, right cold wall and adiabatic horizontal walls. The results are presented in the form of average Nusselt number Figure 2 for $Ra=10^5, 10^6$ and $Da=10^{-3}$, $Pr=5.83$, with different concentration of nanoparticles. It can be seen that the present results are in satisfactory agreement with the numerical results of Sheikhzadeh and Nazari [4].

The second validation is a comparison consists in studying of conjugate natural convection heat transfer in a square porous cavity. It is assumed that the left sidewall is partially heated, the right wall is kept at constant cold temperature and the horizontal walls are insulated. Figure 3 shows the comparisons between the streamlines and the isotherms inside the cavity obtained by the present

code and the results of Al-Farhany and Abdulkadhim [26] for $Ra=10^3$, $D=0.1$, $Kr=1$ and $B=0.2$. The precedent figure predicts a very good agreement between our numerical results and that of Al-Farhany and Abdulkadhim [26].

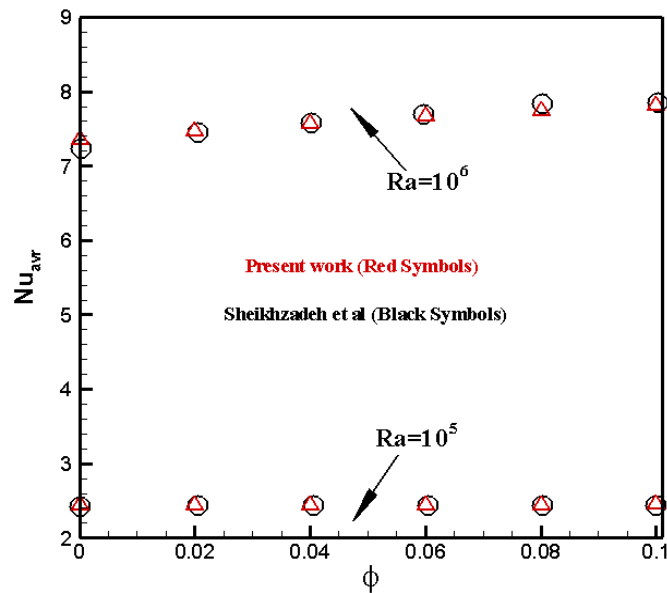


Fig. 2. Validation of average Nusselt number at the heated left wall for $Da=10^{-3}$, $Pr=5.83$

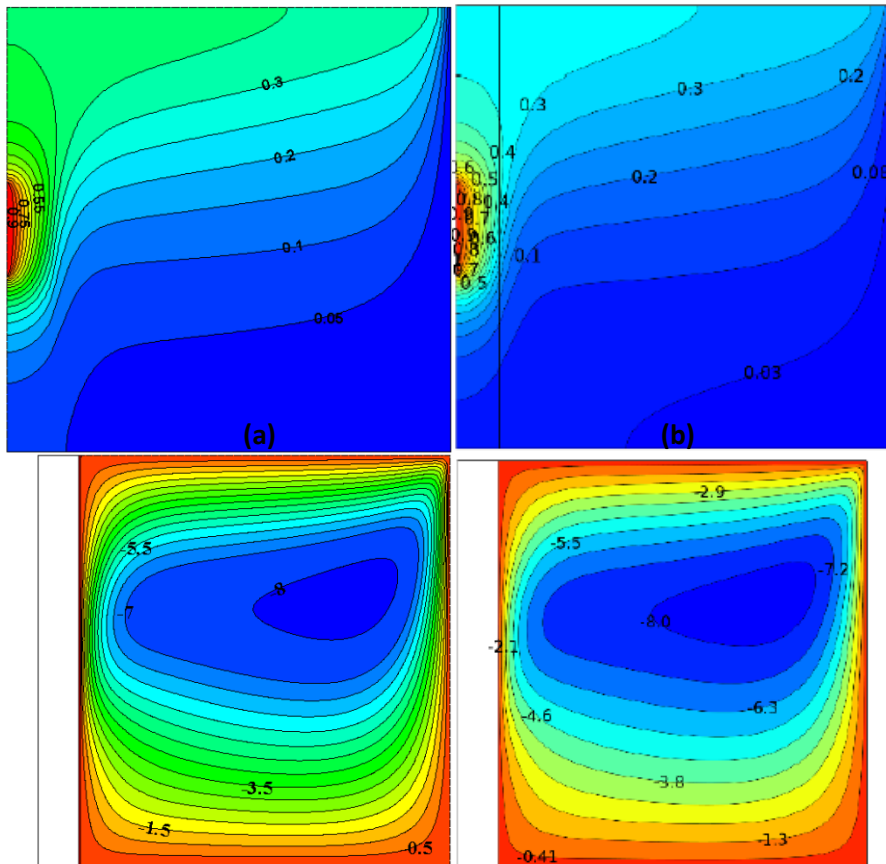


Fig. 3. Isotherms and Streamlines for $Ra=10^3$, $\epsilon=0.1$, $Kr=1$: comparison (a) present results with (b) the result of Al-Farhany and Abdulkadhim [26]

In order to determine a proper grid size for the numerical calculation, grid-independence tests are carried out for the case of $A_h=A_c=0.2$, $L^*=0.5$, $\varphi=8\%$, $Ra=10^7$, $Da=10^{-3}$ and $\varepsilon^*=0.1$. Five different non-uniform grids, namely 832, 1556, 3106, 4170, and 5290 cells are chosen to test the results independency with the grid variation as shown in Table 2. The value of average Nusselt number over the surface of the hot cylinder is used as a measure for comparing numerical accuracy. According to the test performed in Table 2, the optimal mesh chosen is around to 3106 elements.

Table 2

Variation of average Nusselt number with different non-uniform grids

Number of elements	Nu_{avr}
832	11.2632
1556	11.0138
3106	10.9831
4170	10.9811
5290	10.9810

4. Results and Discussion

4.1 Rayleigh and Darcy Number Effects

In this part we have studied the effect of Rayleigh and Darcy Numbers, we fixed the following control parameters: $\varepsilon^*=0.1$, $A_h= A_c=0.2$, $L^*=0.5$ and $\varphi=8\%$. Figure 4 presents the isothermal variation with different values of Rayleigh and Darcy numbers for: (a): $kr=0.5$ and (b): $kr=2$. For any values of Rayleigh and Darcy number, the propagation of heat transfer in the rigid portion is governed by the conductive mode. At $Da=10^{-5}$, the isotherms are nearly parallel between them, which reveal that, pseudo-conduction mechanism dominates the heat transfer in porous-nanofluid layer. Beyond $Ra>10^6$, around the hot source the isotherms have deformed, they are moved to the top (the bottom wall of the conductive obstacle) because the hot fluid expands and loses his density. On the other hand, the cold fluid is relatively dense so it descends from the cold source to the top wall of the solid obstacle. Consequently, we observe the appearance of two layers, one of them hot near the bottom wall of the conductive obstacle and the cold layer is located at top wall of the solid partition, the effect of the thermal boundary layer which becomes clear with increasing Rayleigh number. At $Da=10^{-3}$, the porous medium becomes more permeable to the flow which favor the convective heat transfer. As the number of Rayleigh increases, the exchange becomes more and more important. We note that the thermal boundary layer thickness is contract with the augmentation of Rayleigh and Darcy number. We also observe that the heat exchange has strongly depends on the ratio of thermal conductivity (kr), the elevation of this parameter increases the heat exchange by conduction in the solid obstacle on the one hand. On the other hand, increases convective exchange spontaneously, which demonstrate that the thermal resistance of the solid portion becomes lower, these improve the raise of heat transfer between the two cylinders. For the distribution of the streamlines illustrated in Figure 5, on either side of the enclosure shows that the flow is bicellular and counter-rotating with perfectly symmetrical cells. For low permeability of the porous medium ($Da=10^{-5}$), whatever Rayleigh number the flow intensity has been small, as the resistance of the porous medium is important. Beyond Darcy number equal to 10^{-3} , the flow intensity accentuated with increasing of Rayleigh number, which allows to said, the buoyancy force has been greater than the viscosity effect particularly at $Ra=10^7$. The vortexes keep the same position but they expand towards the rigid walls with the augmentation of the Rayleigh number, as soon as Rayleigh increase, the thickness of the

hydrodynamic boundary layer is reduced, which is clear in the density values of the streamlines near to rigid walls.

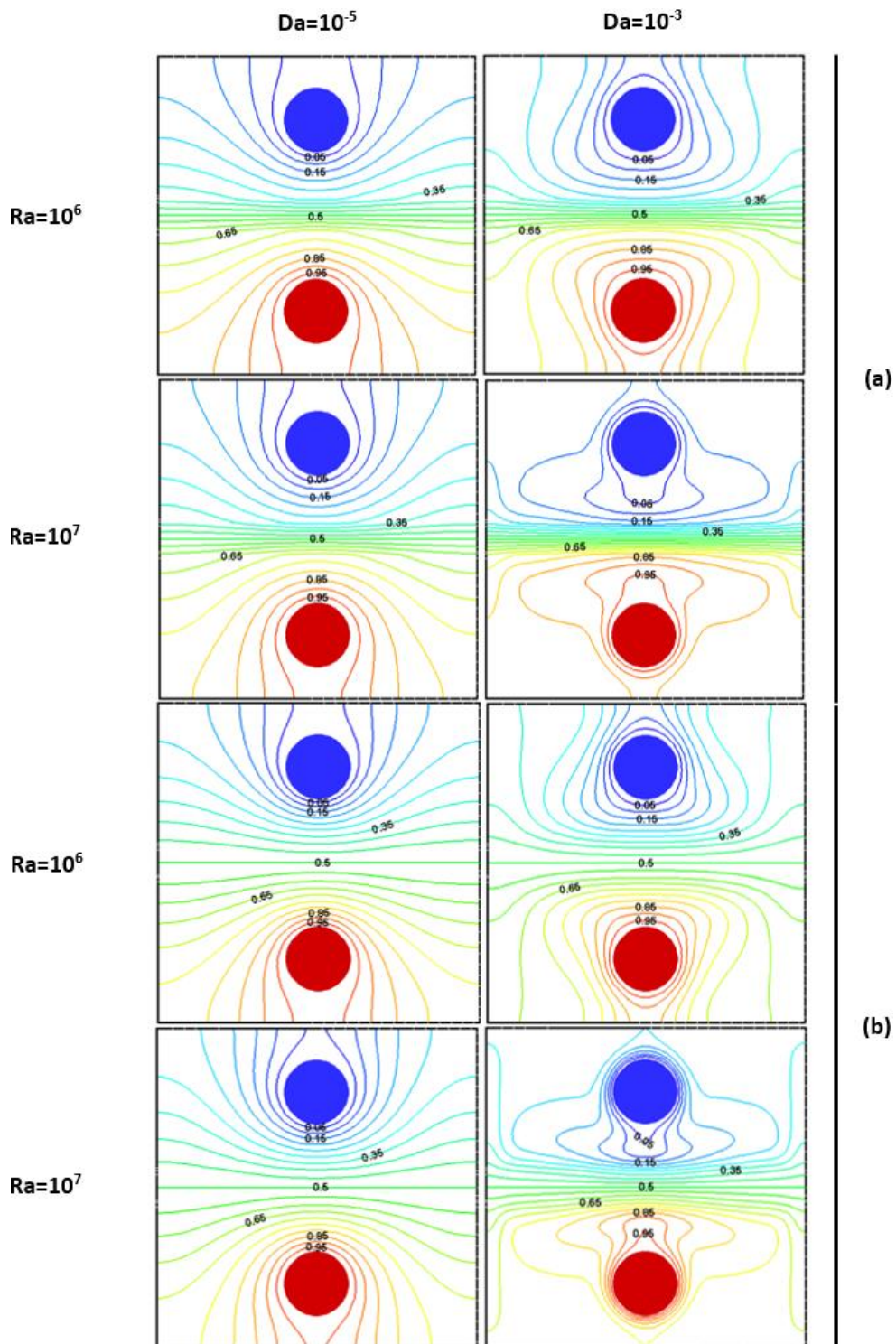


Fig. 4. Isotherms at different Rayleigh and Darcy numbers for $\phi=8\%$, $\epsilon=0.1$: $kr=0.5$ (a) and $kr=2$ (b)

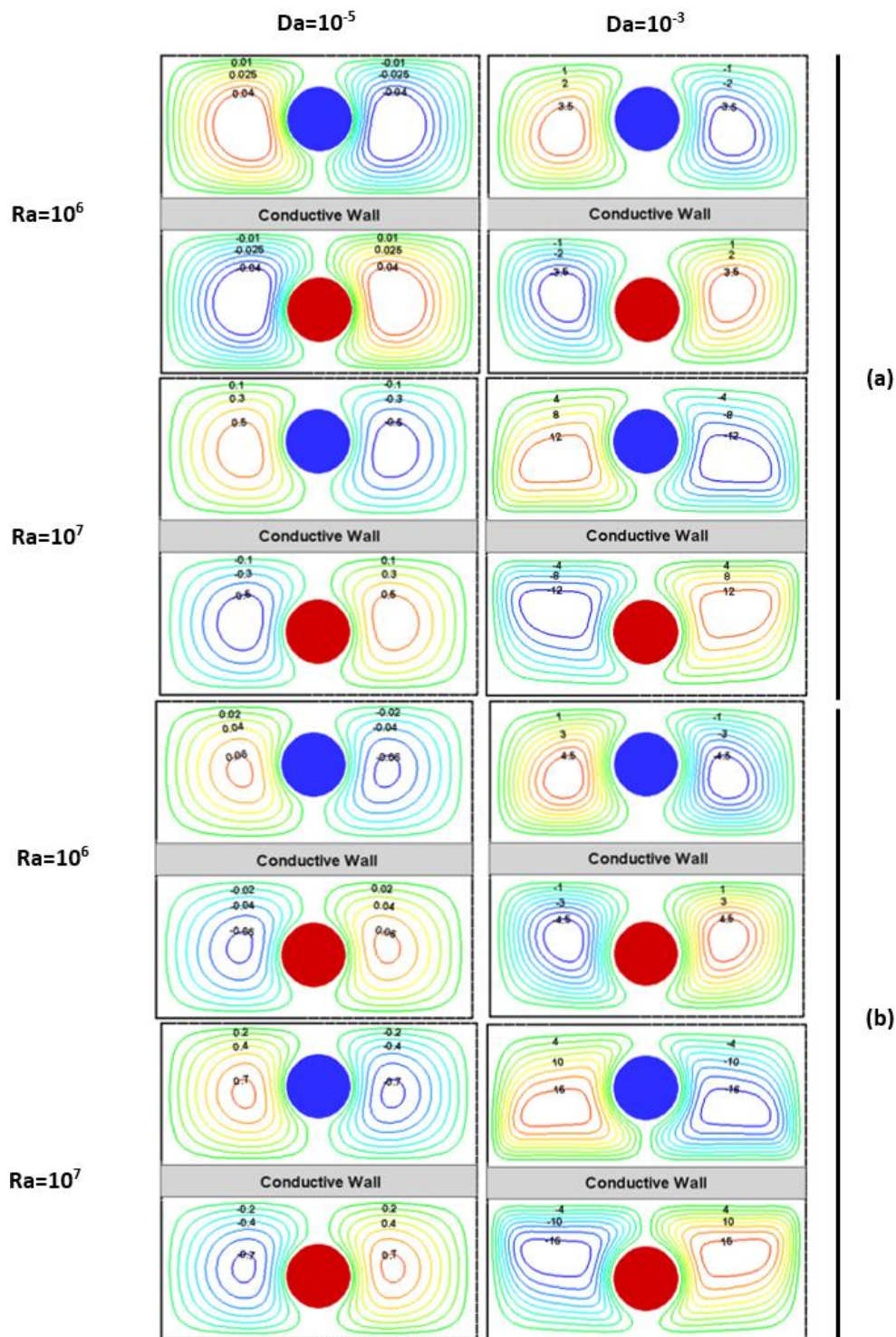


Fig. 5. Streamlines at different Rayleigh and Darcy numbers for $\phi=8\%$, $\epsilon=0.1$: $kr=0.5$ (a) and $kr=2$ (b)

The Figure 6 shows the variation of the local Nusselt number at the bottom wall of the conductive solid. The curves in the figure show a critical point located in the middle of the wall, there is symmetry to this point. Whatever Rayleigh and Darcy number, we note that the heat exchange have been minimal at the lateral borders of the bottom wall. This value expands to the maximal exchange at the middle of the wall, for all cases, the heat transfer rate enhances with increasing of Rayleigh, Darcy number and the conductivity ratio, so the convective heat transfer becomes more important.

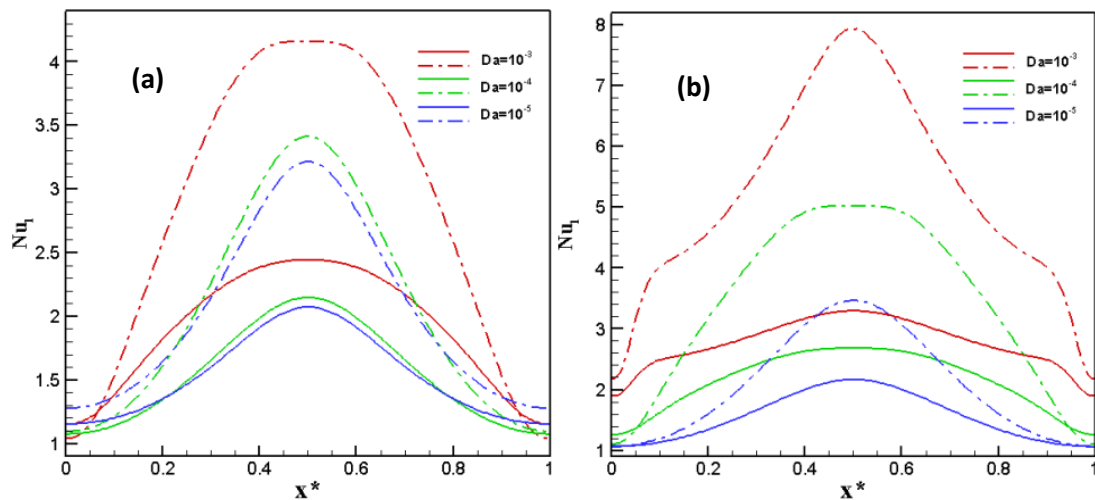


Fig. 6. Profile of local Nusselt number along the bottom wall of the conductive obstacle. Solid lines ($kr=0.5$), Dashed lines ($kr=2$); at different Rayleigh number (a) $Ra=10^6$, (b) $Ra=10^7$

4.2 Dimensionless Wall Thickness Effects

Figure 7 illustrates isotherms and streamlines for different thicknesses of the conducting wall at $Ra = 10^7$, $Da = 10^{-3}$, $A_h = A_c = 0.2$, $L^* = 0.5$, $\phi = 8\%$ and for different values of kr . We remark that the flow intensity becomes strongly with the augmentation of the solid portion thickness, this is due to the porous layer reduction. In addition, we observe a contraction of the internal convective nucleus with the amplification of (ϵ^*) , which favors the conduction heat transfer with comparison to the convective heat exchange. The shape of the isotherms is represented in the Figure 7(a), we see that the hot zone has retracted towards the circular heated wall with increasing of the solid obstacle thickness ϵ^* , for the cold zone the phenomenon is reversed. From this observation, firstly we can say that heat transfer by conduction becomes more dominant; on the other hand, the difference in temperature has decreases with increasing of thermal conductivity ratio. When the thickness of the conductive wall increases, the viscosity effect has been large that the buoyancy forces, therefore, the thickness of the thermal and hydrodynamic boundary layer have developed and consequently heat transfer by conduction is favored. The evolution of the average Nusselt number and the maximum value of the stream function with different thicknesses of the conductive wall are showed in Figure 8. The results show that for different kr values, Nu_{avr} and ψ_{max} decrease with the increasing of ϵ^* in the case of thick and thin partitions. This is due to the reduction of buoyancy forces in comparison with the viscous impact; especially at $kr \leq 0.5$ (in this case the solid partition is practically insulator). The conduction heat transfer in the rigid obstacle is strong that the convective exchange between the two cylindrical sources. It can be seen that the heat exchange becomes almost constant for thick walls with a high value of kr ($kr=10$), the results obtained confirm the previous observations.

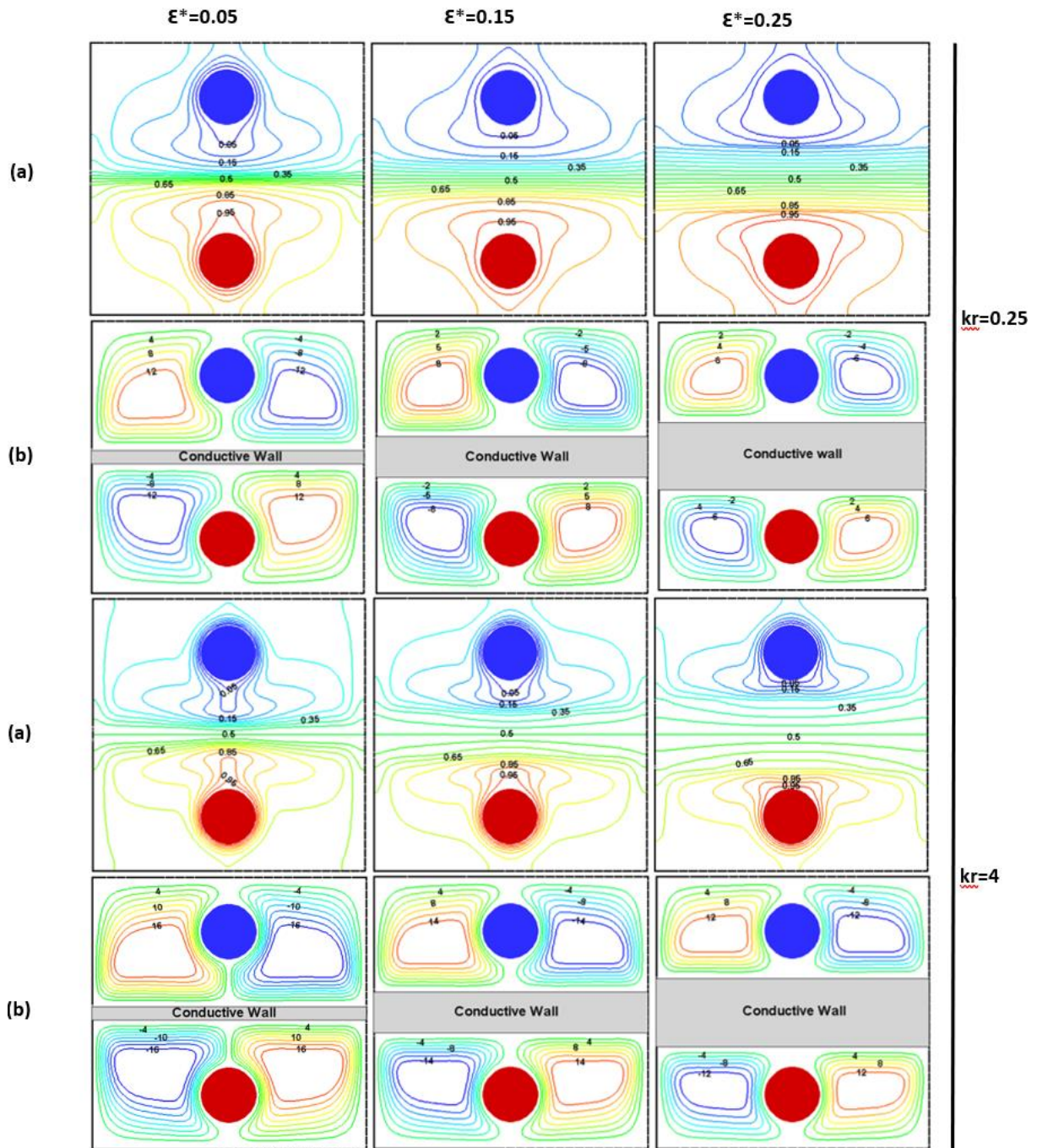


Fig. 7. Isotherms (a) and Streamlines (b) for different wall thickness at $Ra = 10^7$, $Da = 10^{-3}$, $\phi = 8\%$ for $kr = 0.25$ and $kr = 4$

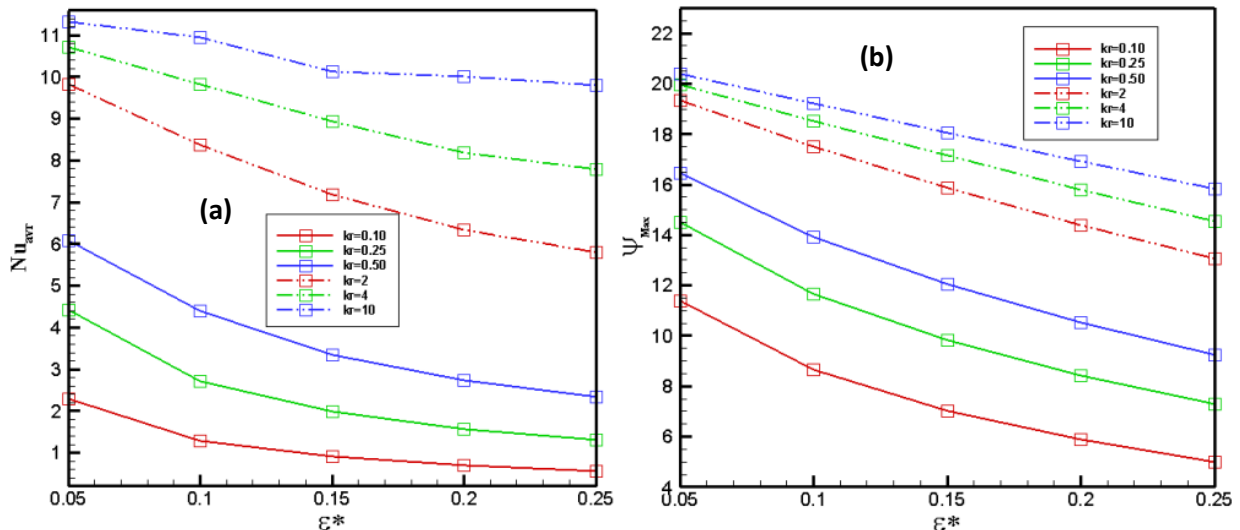


Fig. 8. Variation of the average Nusselt number (a), Maximum stream function value (b) for different values of ϵ^* and kr at $Ra=10^7$, $Da=10^{-3}$, $\phi=8\%$, $L^*=0.5$

4.3 Thermal Conductivity Ratio Effects

To describe the influence of the thermal conductivity ratio on heat transfer in a square porous cavity filled with Al_2O_3/H_2O in the presence of solid portion with different values of Rayleigh and Darcy number, the following parameters are fixed: $\phi=8\%$, $\epsilon^*=0.1$, $A_h=A_c=0.2$, $L^*=0.5$.

Figure 9 shows the variation of the stream function at $x^*=0.2$ and $y^*(0.55; 1)$ for different values of kr . We observe that the curves of stream function are almost parabolic, for all cases the flow intensity near the rigid walls is almost zero, because the effect of viscosity becomes more important that the fluid flow near the bottom layer of the hydrodynamic boundary layer. Moreover, the ψ value expand to the maximum at the center of vortex, obviously the stream function value increases with increasing of Rayleigh and Darcy number, the nanofluid flow intensity at $kr \leq 0.5$ remains slow than $kr > 0.5$.

Therefore, the evolution of the local Nusselt number is represented in Figure 10, the figure illustrates a critical point located in the center of the bottom solid portion, and there is symmetry with respect to this point. The heat exchange is maximal during this point, but it is decreasing to the side borders of the conductive wall. Also, for $kr \leq 0.5$ (the case of a insulate baffles), the local Nusselt number remains almost constant for any value of Rayleigh and Darcy number. As soon as the resistance of conductive wall is higher, the heat exchange between the two cylindrical sources becomes almost non-existent because the thermal conductivity of the solid is poor. When $kr > 0.5$, the Nusselt number increases with the augmentation of Rayleigh and Darcy number, we note that the diversity between the local Nusselt on each value of kr has been remarkable with enhancement of Ra and Da . The influence of kr on buoyancy forces and heat transfer is demonstrated (see Figure 8 and Figure 9), the convective flow has been predominating with the augmentation of Ra , Da and kr .

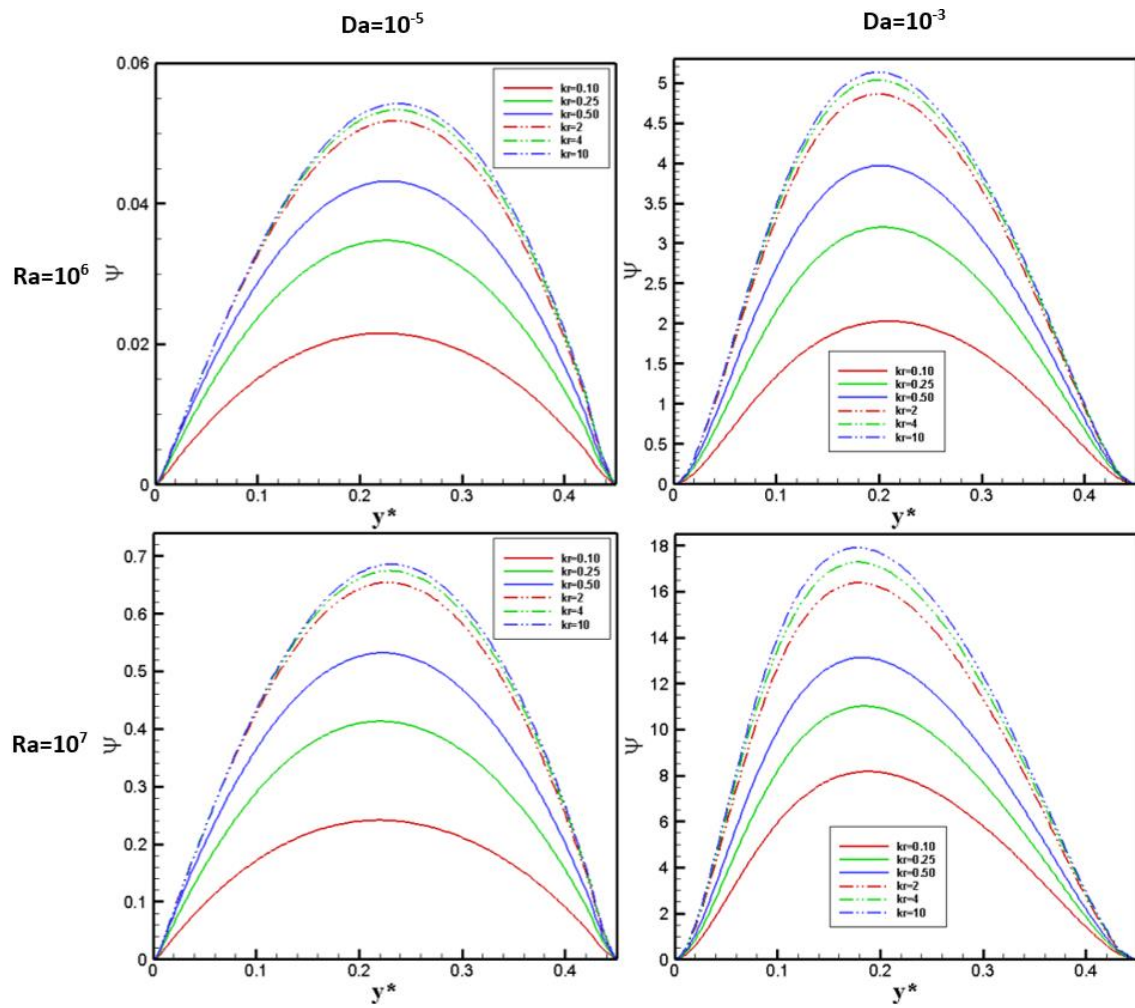


Fig. 9. Variation of the Stream function (ψ) at $x^*=0.2$ and $y^*(0.55;1)$ for different values of kr

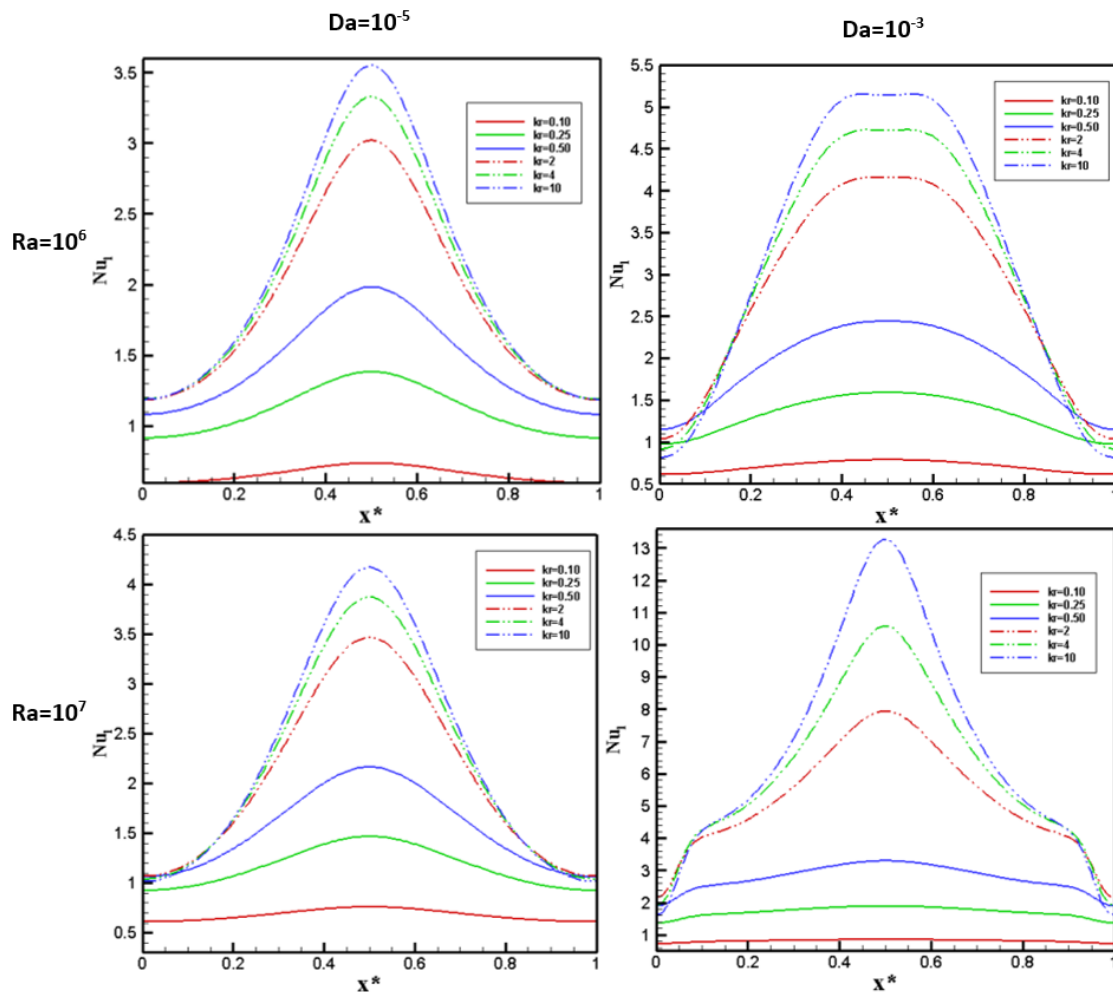


Fig. 10. Variation of local Nusselt number along the bottom wall of the conductive obstacle

4.4 The Nanoparticles Concentration Effects ϕ

In this part we have studied the effect of volume fraction of nanoparticles with different Rayleigh and Darcy number, we fixed the following control parameters: $\epsilon^*=0.1$, $A_H=A_C=0.2$, $L^*=0.5$ and $\phi=8\%$.

The variation of Nu_{avr} as a function of Rayleigh number is illustrated in Figure 11 and Figure 12 for different values of concentration of nanoparticles ϕ . For low permeability Figure 11, whatever the value of Ra, we note that the heat transfer takes a nearly constant value, which indicate that the conductive mode has favored for the most part of the cavity. When ϕ increases, conductive flow improves because the thermal conductivity value of the stagnant nanofluid has been extend. At $Da=10^{-3}$ and for different values of volume fraction of nanoparticles, the average Nusselt number increases as the buoyancy forces in the enclosure are enhanced in the first part, in the other part the rise of the viscous forces decreases the propagation of heat in the cavity. Based on the results obtained in the last figures, we observe that the resistance of porous layer increase with Darcy number decrease and the heat transfer enhancement increase with the permeability of the porous medium augment. At the base's values of thermal conductivity of the conductor solid, the effect of the concentration of nanoparticles is observed to be almost insignificant because the insulation of the solid wall decreases the convective exchange between the two sources. For high values of kr, we note that the average Nusselt number increases with the augmentation in the concentration of nanoparticles, especially to the great values of Rayleigh number.

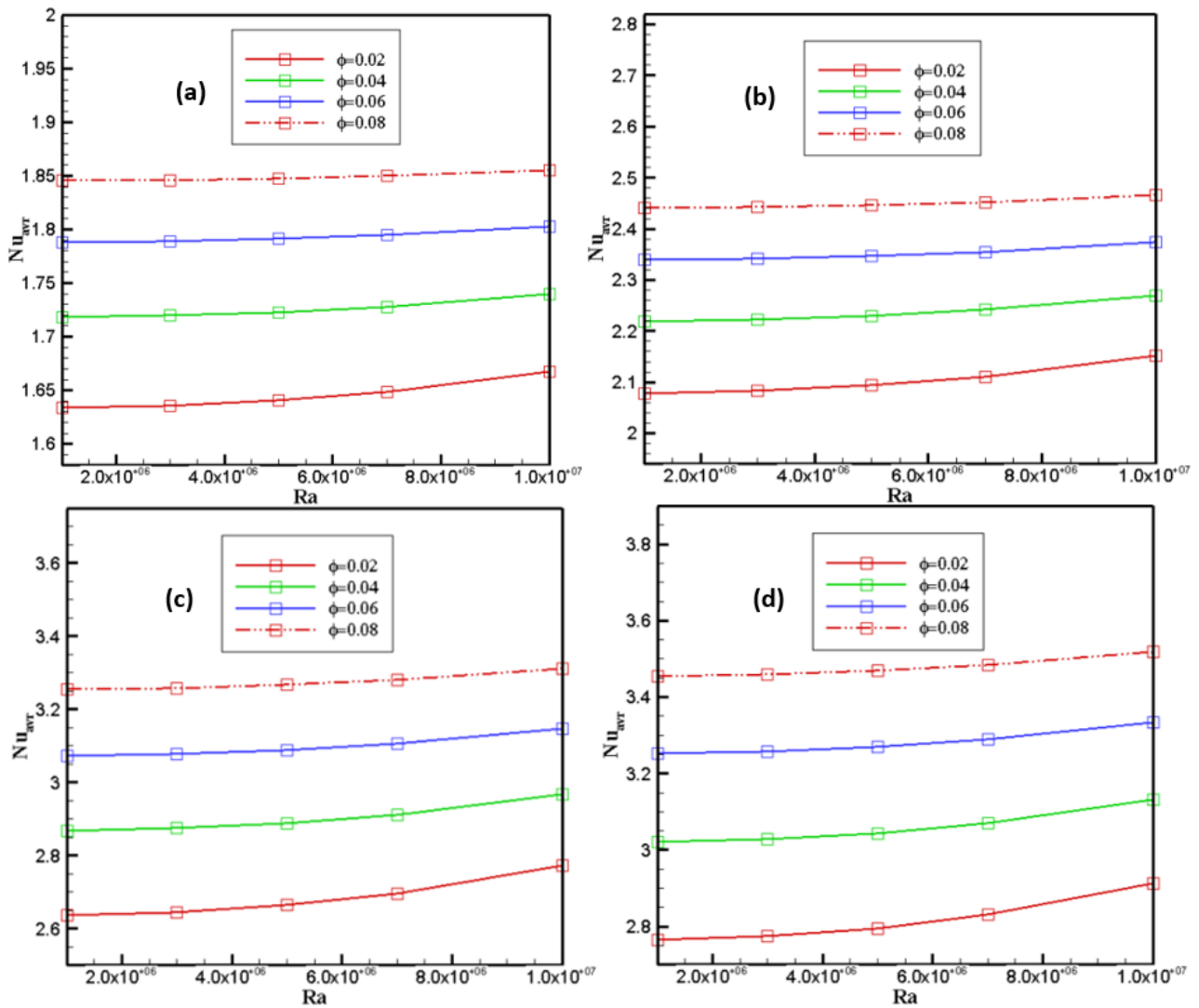


Fig. 11. Variation of Nu_{avr} with various Rayleigh number at $Da=10^{-5}$, $kr=0.25$ (a), $kr=0.5$ (b), $kr=2$ (c), $kr=4$ (d)

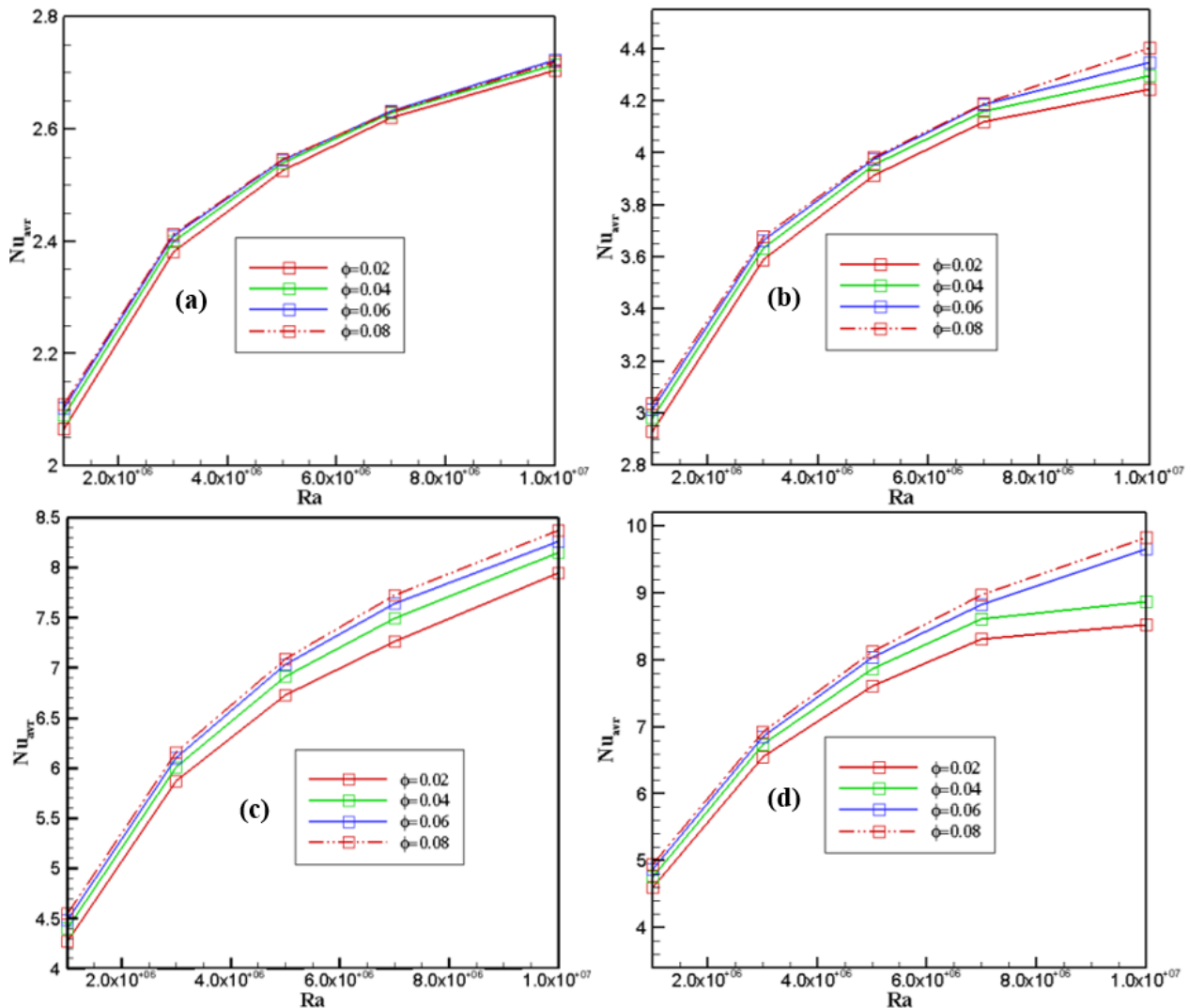


Fig. 12. Variation of Nu_{avr} with various Rayleigh number at $Da=10^{-3}$, $kr=0.25$ (a), $kr=0.5$ (b), $kr=2$ (c), $kr=4$ (d)

5. Conclusions

In the present paper the problem of conjugate natural convection in a square porous cavity saturated with Al_2O_3/H_2O in the presence of two isothermal cylindrical sources was investigated numerically using Galerkin finite element method, the momentum transfer in the porous region is modeled by using Darcy–Brinkman law, the role of conductive wall between two cylindrical sources on the porous layer is originated. The effect of the relevant parameters such as: Rayleigh and Darcy number, concentration of nanoparticles, Thermal conductivity ratio and dimensionless thickness of the solid partition have been investigated and we obtained the following conclusions

- For all considered cases, the heat rate enhances with increasing of Rayleigh number, Darcy number and volume fraction of nanoparticles.
- It is found that, the flow distribution decreases by expanding of rigid partition thickness.
- The heat exchange reduces with the increase in the solid portion thickness but it becomes constant for the thick wall at superior value of thermal conductivity ratio.
- The results show that, the average Nusselt number increase when the conductivity ratio raises, on the other hand the viscous flux improves.
- By increasing the volume fraction, the average Nusselt number improves remarkably. This can be justified by the high value of the thermal conductivity of alumina nanoparticles.

References

- [1] Khanafer, Khalil, and Kambiz Vafai. "Applications of nanofluids in porous medium." *Journal of Thermal Analysis and Calorimetry* 135, no. 2 (2019): 1479-1492.
<https://doi.org/10.1007/s10973-018-7565-4>
- [2] Kasaeian, Alibakhsh, Reza Daneshzarian, Omid Mahian, Lioua Kolsi, Ali J. Chamkha, Somchai Wongwises, and Ioan Pop. "Nanofluid flow and heat transfer in porous media: a review of the latest developments." *International Journal of Heat and Mass Transfer* 107 (2017): 778-791.
<https://doi.org/10.1016/j.ijheatmasstransfer.2016.11.074>
- [3] Bianco, Vincenzo, Oronzio Manca, Sergio Nardini, and Kambiz Vafai, eds. *Heat transfer enhancement with nanofluids*. CRC press, 2015.
<https://doi.org/10.1201/b18324>
- [4] Sheikhzadeh, G. A., and S. Nazari. "Numerical Study of Natural Convection in a Square Cavity Filled with a Porous Medium Saturated with Nanofluid." *Trans. Phenom. Nano Micro Scales* 1, no. 2 (2013): 138-146.
- [5] Baïri, Abderrahmane. "Experimental study on enhancement of free convective heat transfer in a tilted hemispherical enclosure by using Water-ZnO nanofluid saturated porous materials." *Applied Thermal Engineering* 148 (2019): 992-998.
<https://doi.org/10.1016/j.applthermaleng.2018.11.115>
- [6] Aly, Abdelraheem M. "Natural convection over circular cylinders in a porous enclosure filled with a nanofluid under thermo-diffusion effects." *Journal of the Taiwan Institute of Chemical Engineers* 70 (2017): 88-103.
<https://doi.org/10.1016/j.tice.2016.10.050>
- [7] Pop, Ioan, Mohammad Ghalambaz, and Mikhail Sheremet. "Free convection in a square porous cavity filled with a nanofluid using thermal non equilibrium and Buongiorno models." *International Journal of Numerical Methods for Heat and Fluid Flow* 26, no. 3-4 (2016): 671-693.
<https://doi.org/10.1108/HFF-04-2015-0133>
- [8] Groşan, T., C. Revnic, I. Pop, and D. B. Ingham. "Free convection heat transfer in a square cavity filled with a porous medium saturated by a nanofluid." *International Journal of Heat and Mass Transfer* 87 (2015): 36-41.
<https://doi.org/10.1016/j.ijheatmasstransfer.2015.03.078>
- [9] Dogonchi, A. S., M. K. Nayak, Nader Karimi, Ali J. Chamkha, and D. Domiri Ganji. "Numerical simulation of hydrothermal features of Cu-H₂O nanofluid natural convection within a porous annulus considering diverse configurations of heater." *Journal of Thermal Analysis and Calorimetry* (2020): 1-17.
<https://doi.org/10.1007/s10973-020-09419-y>
- [10] Hussain, Salam Hadi, and Mustafa Salah Rahomey. "Comparison of natural convection around a circular cylinder with different geometries of cylinders inside a square enclosure filled with Ag-nanofluid superposed porous-nanofluid layers." *Journal of Heat Transfer* 141, no. 2 (2019).
<https://doi.org/10.1115/1.4039642>
- [11] Sheikholeslami, M., and S. A. Shehzad. "Magnetohydrodynamic nanofluid convection in a porous enclosure considering heat flux boundary condition." *International Journal of Heat and Mass Transfer* 106 (2017): 1261-1269.
<https://doi.org/10.1016/j.ijheatmasstransfer.2016.10.107>
- [12] Sheikholeslami, M., Mikhail A. Sheremet, Ahmad Shafee, and Iskander Tlili. "Simulation of nanofluid thermogravitational convection within a porous chamber imposing magnetic and radiation impacts." *Physica A: Statistical Mechanics and its Applications* (2020): 124058.
<https://doi.org/10.1016/j.physa.2019.124058>
- [13] Ahmed, Sameh E., M. A. Mansour, A. M. Rashad, and T. Salah. "MHD natural convection from two heating modes in finned triangular enclosures filled with porous media using nanofluids." *Journal of Thermal Analysis and Calorimetry* 139, no. 5 (2020): 3133-3149.
<https://doi.org/10.1007/s10973-019-08675-x>
- [14] Lavanya, Bommanna, and Madduleti Nagasasikala. "Effects of Dissipation and Radiation on Heat Transfer Flow of a Convective Rotating Cu-Water Nano-fluid in a Vertical Channel." *Journal of Advanced Research in Fluid Mechanics and Thermal Sciences* 50, no. 2 (2018): 108-117.
- [15] Zokri, Syazwani Mohd, Sidra Aman, Zulkhibri Ismail, Mohd Zuki Salleh, and Ilyas Khan. "Effect of MHD and porosity on exact solutions and flow of a hybrid Casson-nanofluid." *Journal of Advanced Research in Fluid Mechanics and Thermal Sciences* 44, no. 1 (2018): 131-139.
- [16] Chamkha, Ali J., and Muneer A. Ismael. "Conjugate heat transfer in a porous cavity filled with nanofluids and heated by a triangular thick wall." *International Journal of Thermal Sciences* 67 (2013): 135-151.
<https://doi.org/10.1016/j.ijthermalsci.2012.12.002>

- [17] Ismael, Muneer A., T. Armaghani, and Ali J. Chamkha. "Conjugate heat transfer and entropy generation in a cavity filled with a nanofluid-saturated porous media and heated by a triangular solid." *Journal of the Taiwan Institute of Chemical Engineers* 59 (2016): 138-151.
<https://doi.org/10.1016/j.jtice.2015.09.012>
- [18] Alsabery, Ammar I., Muneer A. Ismael, Ali J. Chamkha, and Ishak Hashim. "Impact of finite wavy wall thickness on entropy generation and natural convection of nanofluid in cavity partially filled with non-Darcy porous layer." *Neural Computing and Applications* (2020): 1-21.
<https://doi.org/10.1007/s00521-020-04776-z>
- [19] Sheremet, Mikhail Alexandrovich, and Ioan Pop. "Conjugate natural convection in a square porous cavity filled by a nanofluid using Buongiorno's mathematical model." *International Journal of Heat and Mass Transfer* 79 (2014): 137-145.
<https://doi.org/10.1016/j.ijheatmasstransfer.2014.07.092>
- [20] Mehryan, S. A. M., Mohsen Izadi, and Mikhail A. Sheremet. "Analysis of conjugate natural convection within a porous square enclosure occupied with micropolar nanofluid using local thermal non-equilibrium model." *Journal of Molecular Liquids* 250 (2018): 353-368.
<https://doi.org/10.1016/j.molliq.2017.11.177>
- [21] Ghalambaz, Mohammad, Mikhail A. Sheremet, S. A. M. Mehryan, Farshad M. Kashkooli, and Ioan Pop. "Local thermal non-equilibrium analysis of conjugate free convection within a porous enclosure occupied with Ag-MgO hybrid nanofluid." *Journal of Thermal Analysis and Calorimetry* 135, no. 2 (2019): 1381-1398.
<https://doi.org/10.1007/s10973-018-7472-8>
- [22] Tahmasebi, Ali, Mahboobe Mahdavi, and Mohammad Ghalambaz. "Local thermal nonequilibrium conjugate natural convection heat transfer of nanofluids in a cavity partially filled with porous media using Buongiorno's model." *Numerical Heat Transfer, Part A: Applications* 73, no. 4 (2018): 254-276.
<https://doi.org/10.1080/10407782.2017.1422632>
- [23] Mehryan, S. A. M., Mohammad Ghalambaz, and Mohsen Izadi. "Conjugate natural convection of nanofluids inside an enclosure filled by three layers of solid, porous medium and free nanofluid using Buongiorno's and local thermal non-equilibrium models." *Journal of Thermal Analysis and Calorimetry* 135, no. 2 (2019): 1047-1067.
<https://doi.org/10.1007/s10973-018-7380-y>
- [24] Ismael, Muneer A., and Ali J. Chamkha. "Conjugate natural convection in a differentially heated composite enclosure filled with a nanofluid." *Journal of Porous Media* 18, no. 7 (2015).
<https://doi.org/10.1615/JPorMedia.v18.i7.50>
- [25] Doha, Mohammed, Draoui Belkacem, Abdellah Belkacem, and Amina Saber. "Numerical Simulation of Natural Convection in a Square Cavity with Two Partitions and Two Fluids." *International Review of Mechanical Engineering* 12, no. 3 (2018): 223.
<https://doi.org/10.15866/ireme.v12i3.14669>
- [26] Al-Farhany, Khaled, and Ammar Abdulkadhim. "Numerical investigation of conjugate natural convection heat transfer in a square porous cavity heated partially from left sidewall." *International Journal of Heat and Technology* 36, no. 1 (2018): 237-244.
<https://doi.org/10.18280/ijht.360132>